Research article

Curcumin protects mice with myasthenia gravis by regulating the gut microbiota, short-chain fatty acids, and the Th17/Treg balance

Jing Sun [a],[1], Qinfang Xie [a],[1], Mengjiao Sun [a], Wenjing Zhang [b], Hongxia Wang [a], Ning Liu [a], Manxia Wang [a],*

[a] Department of Neurology, Lanzhou University Second Hospital, Lanzhou, Gansu, 730030, China
[b] Department of Neurology, Qinghai Provincial People's Hospital, Xining, Qinghai, 810007, China

ARTICLE INFO

ABSTRACT

Curcumin is widely used as a traditional drug in Asia. Interestingly, curcumin and its metabolites have been demonstrated to influence the microbiota. However, the effect of curcumin on the gut microbiota in patients with myasthenia gravis (MG) remains unclear. This study aimed to investigate the effects of curcumin on the gut microbiota community, short-chain fatty acids (SCFAs) levels, intestinal permeability, and Th17/Treg balance in a Torpedo acetylcholine receptor (T-AChR)-induced MG mouse model. The results showed that curcumin significantly alleviated the clinical symptoms of MG mice induced by T-AChR. Curcumin modified the gut microbiota composition, increased microbial diversity, and, in particular, reduced endotoxin-producing Proteobacteria and Desulfovibrio levels in T-AChR-induced gut dysbiosis. Moreover, we found that curcumin significantly increased fecal butyrate levels in mice with T-AChR-induced gut dysbiosis. Butyrate levels increased in conjunction with the increase in butyrate-producing species such as Oscillospira, Akkermansia, and Allobaculum in the curcumin-treated group. In addition, curcumin repressed the increased levels of lipopolysaccharide (LPS), zonulin, and FD4 in plasma. It enhanced Occludin expression in the colons of MG mice induced with T-AChR, indicating dramatically alleviated gut permeability. Furthermore, curcumin treatment corrected T-AChR-induced imbalances in Th17/Treg cells. In summary, curcumin may protect mice against myasthenia gravis by modulating both the gut microbiota and SCFAs, improving gut permeability, and regulating the Th17/Treg balance. This study provides novel insights into curcumin's clinical value in MG therapy.

1. Introduction

Myasthenia gravis (MG) is an autoimmune disorder caused by antibodies that attack the acetylcholine receptor (AChR), muscle-specific kinase (MuSK), and low-density lipoprotein receptor-related protein 4 (LRP4) [1], among which AChR-related MG accounts for 85% of all cases [2]. These antibodies disrupt the neuromuscular junction (NMJ) and interfere with neuromuscular transmission, resulting in weakness and fatigue of the skeletal muscles [2]. MG's estimated global incidence rate ranges from 0.3 to 2.8/100000, with a median value of 10/100000 [3,4]. In China, the incidence rate of MG is 0.68/100000. Specifically, the incidence

---

Abbreviations

MG	Myasthenia gravis
EAMG	experimental autoimmune myasthenia gravis
SCFAs	Short-chain fatty acids
I-FABP	intestinal fatty acid binding protein
LPS	lipopolysaccharide
FD4	FITC-dextran 4 kDa
AChR	acetylcholine receptor
MuSK	muscle-specific kinase
LRP4	low-density lipoprotein receptor-related protein 4
Th17	T-helper 17
Treg	T-regulatory
T-AChR	Torpedo californica AChR
CFA	Complete Freund's Adjuvant
IFA	Incomplete Freund's Adjuvant
DMSO	dimethyl sulfoxide
OFT	open field test
PCoA	principal main coordinate analysis
TGF-ncipal main coordinate analysis; sis; ai	

rate among females is 0.76 per 100,000, while among males it is 0.60 per 100,000. Notably, the incidence rate in women exhibits a slightly higher proportion [5]. Corticosteroids are generally recommended for induction as well as immunosuppressants for maintenance, patients with severe cases and acute worsening require intravenous immunoglobulin or plasmapheresis as well [6]. In approximately 15% of patients with refractory MG, complete control of the disease is not possible or is only possible with the severe side effects of immunosuppressive therapy [7]. In order to address this issue, we urgently need new drugs with fewer side effects and better efficacy. Traditional Chinese herbal medicine has shown good results in this area recently.

Numerous factors are associated with MG, including genes, environment, and immunity; the environmental factors mainly include hormones, microbiota, vitamin D, and diet [8,9]. The gut microbiome plays an important role in the maintenance of homeostasis of the immune system and the pathogenesis of autoimmune diseases [10]. Numerous studies have demonstrated that the gut microbiota can affect the Th17/Treg cell balance [11–13]. Segmented filamentous bacteria secreted by intestinal bacteria are major factors that drive the differentiation of Th17 cells [14]. Moreover, metabolites, especially SCFAs, which are produced by gut microbiota, influence Treg induction [15–17]. A growing body of evidence indicates that anti-inflammatory T-regulatory (Treg) cells and pro-inflammatory T-helper 17 (Th17) cells interact antagonistically, contributing to MG pathogenesis [2,18–20]. Several previous studies have explored how the gut microbial composition changes in MG patients, and these studies present diverse findings. Qiu et al. [21] revealed that patients with MG had less microbial diversity and different community structures. Patients with MG were reported to have lower total SCFA content than the healthy control (HC) population, with noticeably lower propionate and butyrate levels. In another study [22], it was discovered that patients with MG had considerably higher concentrations of Pasteurellaceae, Desulfovibrionaceae, and Acidaminococcaceae than HCs. MG patients also exhibited significantly lower relative abundances of Bifdobacteraceae and Verrucomicrobiaceae, along with Leuconostocaccaceae, Flavobacteraceae, and Coriobacteraceaes. Zheng et al. [23] found that patients with MG had higher relative abundances of Bacteroidetes and Fusobacteria, whereas Actinobacteria were less abundant. Tan et al. [24] also found that patients with distinct MG subtypes had variable gut flora, which in turn resulted in variable fecal metabolic contents. Therefore, effective interventions targeting gut microbiota may be part of the most promising strategies to alleviate MG.

Curcumin is an effective constituent of the traditional Asian medicine turmeric with antioxidant, anti-inflammatory and neuroprotective properties [25]. Curcumin has been reported to alleviate the clinical symptoms of MG rats by modulating immune cells [26]. Of note, curcumin has been recently proposed for the management of neurological diseases by regulating the gut microbiota and improving gut barrier function [27–29]. It was reported that curcumin could considerably alter the ratio of pathogenic and beneficial bacteria by reducing the relative abundance of genera including *Prevotellaceae, Coriobacterales, Enterobacteria*, and *Enterococci* while increasing the relative abundance of favorable genera including *Bifidobacteria* and *Lactobacilli* [30]. Hence, curcumin seems to have promising clinical applications. However, its precise mechanisms of pharmacological action remain unclear. Furthermore, the effects of curcumin on intestinal mucosal barriers and intestinal flora in MG patients have not been explored in detail.

In the present study, *Torpedo californica* AChR (T-AChR) was used to induce a MG mouse model. We found that curcumin alleviated the clinical symptoms, corrected the microbiota imbalance, increased SCFA-producing bacteria, reduced intestinal permeability, and regulated the Th17/Treg balance in T-AChR-induced MG mice. Thus, our results provide novel insights into curcumin's clinical value in MG therapy.

2. Results

2.1. Curcumin ameliorated the clinical presentation of T-AChR-induced MG mice

T-AChR was administered to induce EAMG in C57BL/6J mice, and curcumin was given by gavage to treat EAMG (Fig. 1A). The body weight was different among the groups. Compared to the controls, the body weight of EAMG mice decreased ($P < 0.05$) ; however, the body weights increased ($P < 0.001$) after receiving curcumin treatment for 4 weeks (Fig. 1B). In addition, EAMG mice had higher ($P < 0.001$) Lennon scores than the controls, and Lennon scores were decreased ($P < 0.01$) in the curcumin-treated group (Fig. 1C). The OFT was used to evaluate the impact of curcumin on MG-related locomotion (Fig. 1D), and it was found that the overall journey distance (OJD) of the EAMG mice was significantly reduced compared to that of the controls ($P < 0.001$, Fig. 1E); the OJD was significantly increased in the curcumin-treated mice ($P < 0.05$, Fig. 1E). These findings suggested that curcumin can ameliorate the severity of T-AChR-induced MG in mice.

2.2. Correlation between the Lennon score and microorganisms, metabolism, intestinal barrier markers, and serum markers

In order to delve deeper into the connections between disruptions in the gut microbiome, fecal metabolome, intestinal barrier markers, serum markers, and the clinical severity of EAMG mice, a correlation analysis was conducted. The results revealed a significant positive correlation between the Lennon score and serum IL-17A level, as well as a negative correlation with serum IL-10 level and the relative abundance of genus *Oscillospira*. However, no significant correlation was observed with other indicators. These findings imply that MG is characterized by disturbances in both gut microbiome and cytokines (Table 1).
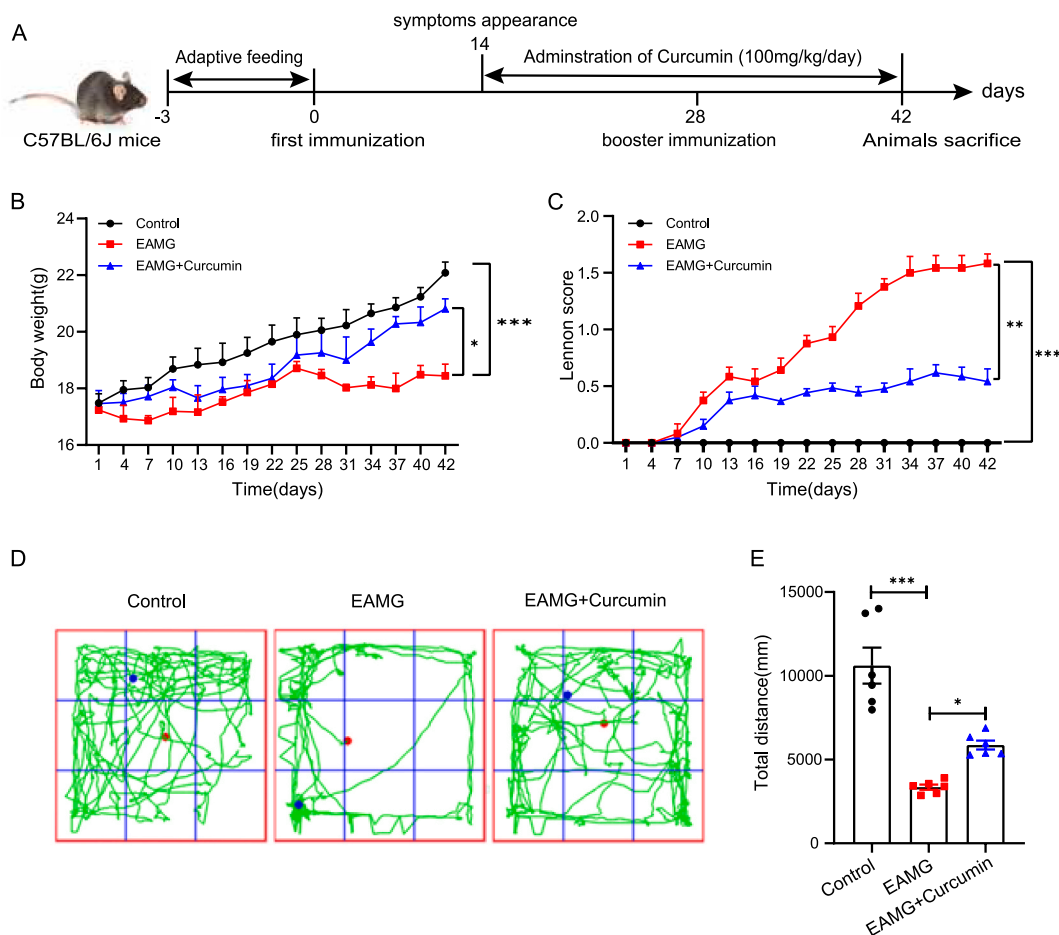

Fig. 1. Curcumin remarkably alleviated T-AChR-induced MG in mice. (A) Diagram for experimental schedule. (B) The body weight, (C) The Lennon score, (D) Representative motion tracks for "healthy" mice (Control), "MG" mice (EAMG), and curcumin treat mice (EAMG + Curcumin). (E) The total motion distance of EAMG was substantially decreased compared to that in control mice and was increased in the curcumin treat mice (n = 6/group). Data presented as means ± SEM. *$P < 0.05$, **$P < 0.01$, and ***$P < 0.001$.

Table 1
Correlation between the Lennon score and microorganisms, metabolism, intestinal barrier markers, and serum markers.

	Lennon score	
	r	P valve
Proteobacteria	0.5176	0.2929
Desulfovibrio	0.5319	0.2774
Oscillospira	−0.8616	0.0274
Allobaculum	0.0461	0.9310
Akkermansia	−0.1486	0.7787
Acetic acid	−0.0842	0.8740
Butyric acid	0.0170	0.9745
FD4	0.3825	0.4778
LPS	0.2452	0.6396
I-FABP	0.6976	0.1233
Zonulin	0.4264	0.3992
Occludin	−0.3109	0.7987
ZO-1	−0.3449	0.7758
IL-6	0.4090	0.4207
IL-17A	0.9496	0.0037
IL-23	−0.0773	0.8843
IL-10	−0.8651	0.0261
TGF-β1	0.3250	0.5297

P-values of <0.05 are considered statistically significant.
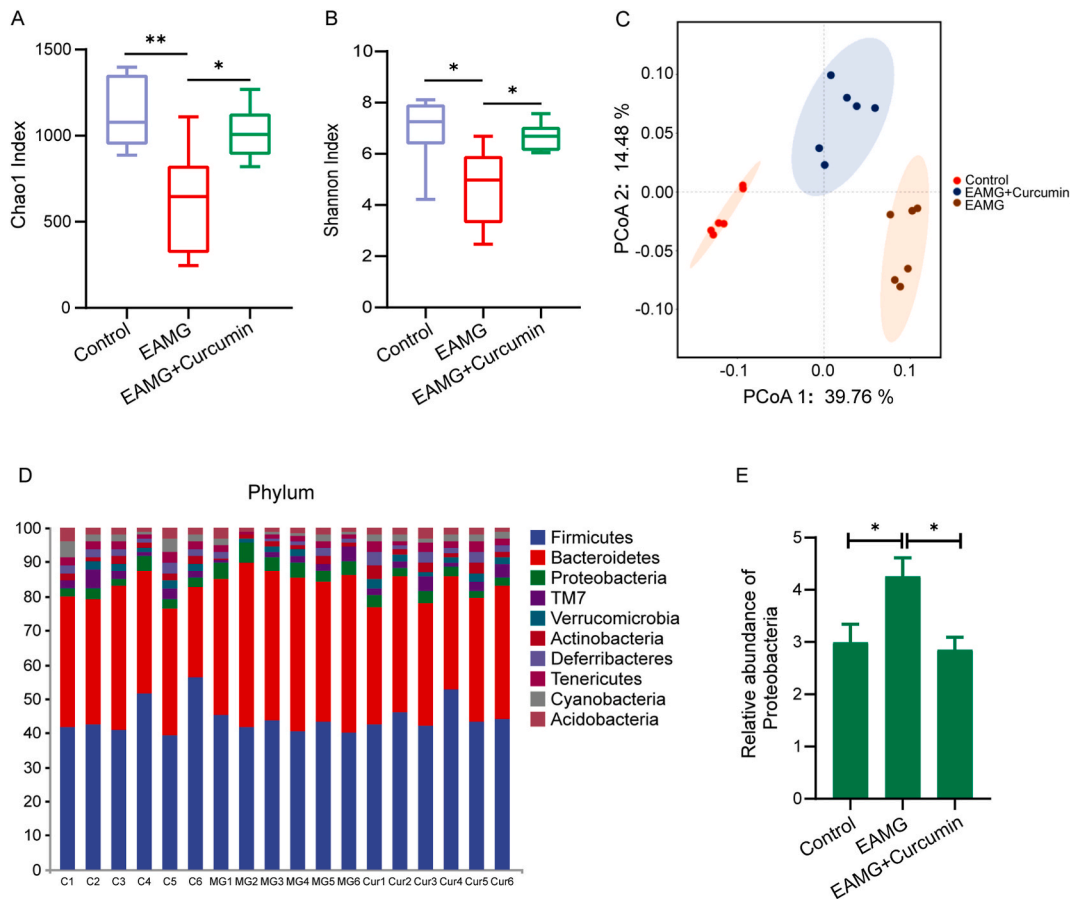
Fig. 2. Curcumin altered the gut microbiota diversity and composition. (A) Chao I and (B) Shannon indexes were assessed for the comparison of alpha diversity. (C) PCoA of the fecal microbial communities based on unweighted UniFrac. (D) Top 10 abundance of the microbial community in phylum level. (E) The relative abundance of Proteobacteria. (A–E) (n = 6/group). Each symbol represents an individual mouse. *$P < 0.05$, **$P < 0.01$.

2.3. Curcumin altered the composition of the gut microbiota in T-AChR-induced MG mice

The gut microbiome of the mice in each group was sequenced and analyzed. Compared to controls, the enhanced Chao1 and Shannon index was significantly reduced in the EAMG group but evidently increased in the curcumin group, which means that curcumin treatment could significantly affect the gut microbial diversity of the mice (both $P < 0.05$, Fig. 2A and B). Principal coordinates analysis (PCoA) using UniFrac distances further demonstrated that there was an obvious difference in the gut microbiome among the groups (Fig. 2C). We then studied the different phyla and genera among the groups (Figs. 2D and 3A). The relative abundance of Proteobacteria was obviously increased in the EAMG group but clearly reduced in the curcumin group (Fig. 2E). Four genera were significantly changed among the groups. The relative abundances of *Oscillospira* ($P < 0.001$), *Allobaculum* ($P < 0.05$), and *Akkermansia* ($P < 0.01$) were significantly decreased in the EAMG group, but increased in the curcumin group ($P < 0.01$, $P < 0.05$, $P < 0.05$, Fig. 3E–G). However, the relative abundance of *Desulfovibrio* was significantly increased in the EAMG group and decreased in the curcumin group (both $P < 0.05$, Fig. 3D). Based on these results, curcumin is capable of correcting gut dysbiosis caused by T-AChR.

2.4. Curcumin changed SCFAs in T-AChR-induced MG mice

Considering the protective effect of curcumin on the gut microbiota and the regulation of immune responses by SCFAs, we evaluated the concentrations of SCFAs in the feces by using GC−MS. In the T-AChR-induced EAMG group, fecal acetic acid and butyric acid concentrations were decreased, whereas curcumin administration reversed this reduction (Fig. 3B–C) (Table 2). These changes may be directly correlated to the abundance of the genera *Oscillospira*, *Akkermansia*, and *Allobaculum* (Fig. 3E–G).

2.5. Curcumin reduced intestinal permeability in T-AChR-induced MG mice

Based on the above findings, we further investigated the intestinal permeability in each group. Altered intestinal permeability contributes to a variety of diseases and serves as an indicator of intestinal barrier integrity [31]. Therefore, intestinal permeability was also measured to indirectly reflect the effect of curcumin on the regulation of dysbiosis induced by T-AChR. First, intestinal permeability was determined by the extravasation of FITC-dextran 4 kDa. Fig. 4A indicates that plasma FITC-dextran 4 kDa was significantly increased 4 h after administration in the EAMG group compared with controls ($P < 0.001$). Curcumin dramatically reduced the
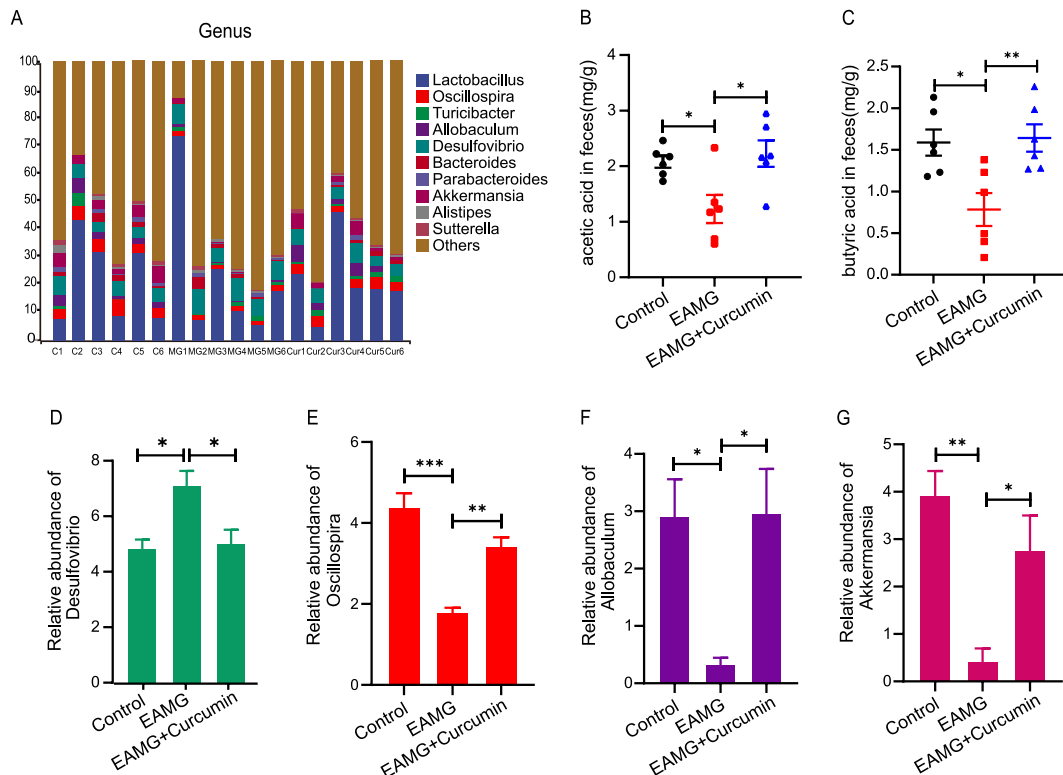

Fig. 3. Curcumin modulated the gut microbiota and increased the abundance of SCFA-producing bacteria. (A) Fecal microbiota composition at the genus level. (B–C) GC–MS quantification of acetic acid and butyric acid levels in cecal contents. (D–G) The relative abundance of *Desulfovibrio*, *Oscillospira*, *Allobaculum*, and *Akkermansia*. All results are from three independent experiments and expressed as the mean ± SEM (n = 6/group), *$P < 0.05$, **$P < 0.01$, and ***$P < 0.001$.

Table 2

SCFAs concentrations (mg/g) of three group mice feces.

| SCFAs	Control	EAMG	EAMG + Curcumin
Acetic acid	2.080 ± 0.107	1.229 ± 0.252[A]	2.227 ± 0.237 [B]
Propionic acid	0.521 ± 0.059	0.442 ± 0.029	0.494 ± 0.090
Butyric acid	1.588 ± 0.157	0.783 ± 0.197[A]	1.643 ± 0.165 [C]
Isobutyric acid	0.025 ± 0.004	0.023 ± 0.004	0.014 ± 0.004
Isovaleric acid	0.011 ± 0.001	0.011 ± 0.002	0.012 ± 0.003
Valeric acid	0.057 ± 0.006	0.057 ± 0.013	0.042 ± 0.012
Total SCFAs	4.282 ± 0.334	2.545 ± 0.497	4.432 ± 0.511

Data were expressed as mean ± SEM (n = 6/group). [A] compared to the Control group ($P < 0.05$), [B] compared to the EAMG group ($P < 0.05$), [C] compared to the EAMG group ($P < 0.01$).
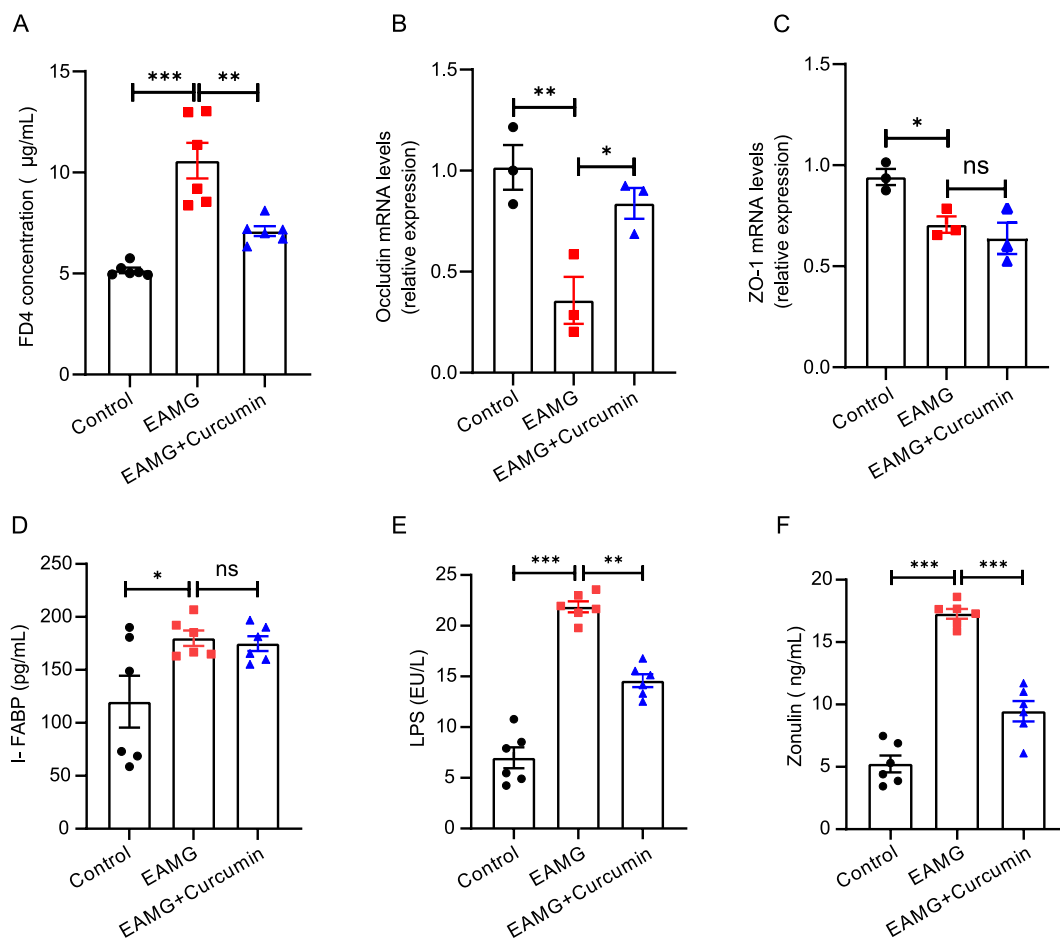
Fig. 4. Curcumin improved the gut permeability in T-AChR-induced MG mice. (A) Epithelial permeability. Mice were orally administrated with FITC-labeled dextran (44 mg/100g body weight). Serum was collected 4h later and fluorescence intensity was determined. (B–C) MRNA expression levels of Occludin and ZO-1 by real-time PCR. (D) Plasma I-FABP. (E) Plasma LPS. (F) Plasma zonulin. Data were presented as mean ± SEM (n = 6/group). *$P < 0.05$, **$P < 0.01$, ***$P < 0.001$, ns = not significant.

enhancement of intestinal permeability induced by T-AChR ($P < 0.01$). In addition, we analyzed the expression of genes associated with intestinal epithelial tight junctions, and our results showed that Occludin expression was significantly downregulated in the EAMG group ($P < 0.01$), while curcumin significantly increased Occludin expression ($P < 0.05$) (Fig. 4B). ZO-1 expression was not significantly different between the EAMG and curcumin groups (Fig. 4C). Moreover, the potential role of curcumin in the regulation of intestinal permeability was further examined by detecting the levels of plasma I-FABP, LPS, and zonulin. The levels of LPS (Fig. 4E, $P < 0.001$) and zonulin (Fig. 4F, $P < 0.001$) were significantly increased in EAMG mice and decreased after treatment with curcumin. However, the level of I-FABP showed no significant changes between the EAMG and curcumin groups (Fig. 4D). Overall, our findings showed that intestinal permeability was increased in T-AChR-induced MG mice, but permeability could be reduced by treatment with
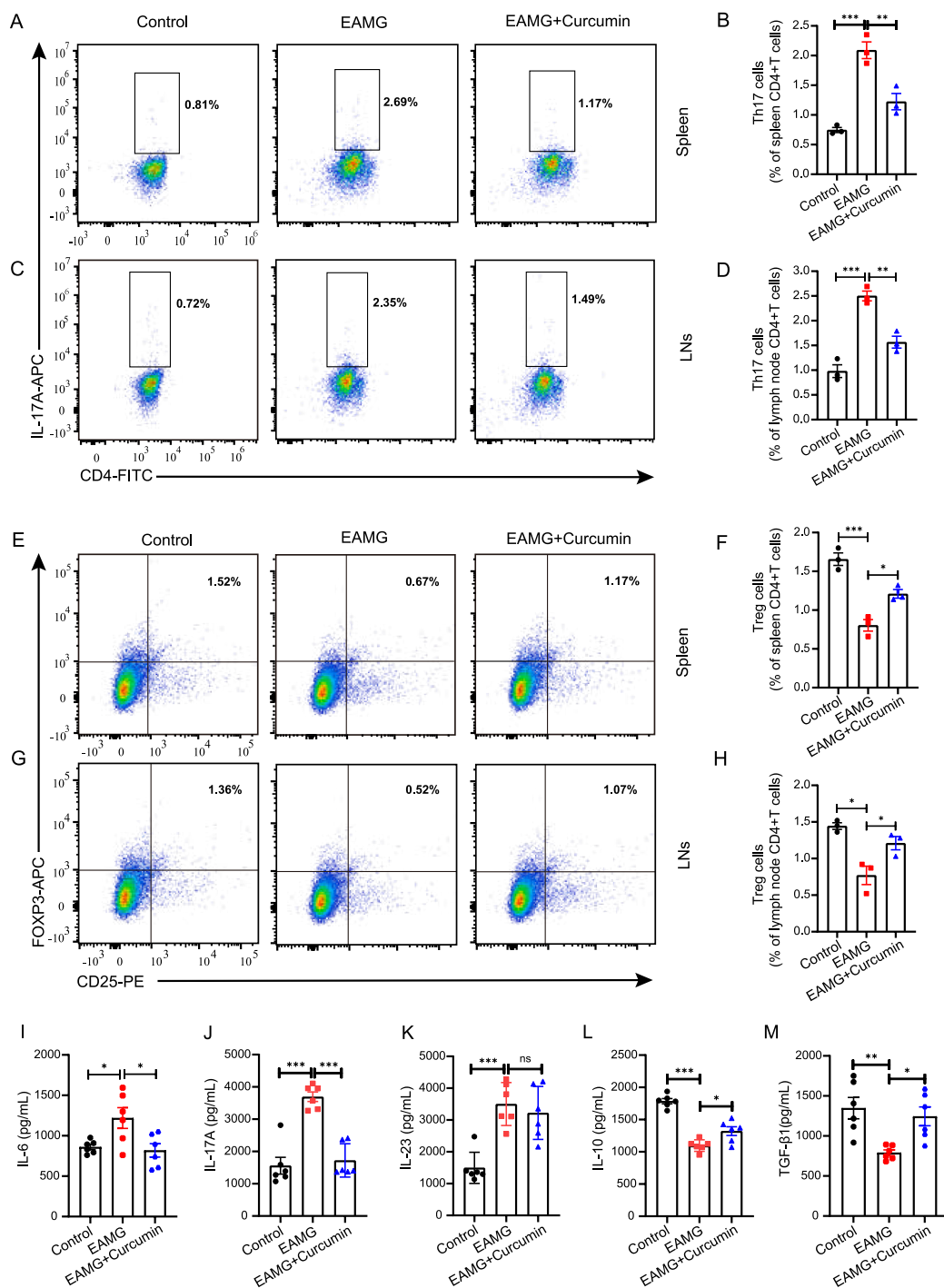
Fig. 5. Curcumin regulated the Th17/Treg balance in the spleen and inguinal lymph nodes. Flow cytometry for IL-17A (Th17) expression in (A) spleens and (C) inguinal lymph nodes of the control, EAMG, and curcumin-treated group (n = 3/group). Frequencies of CD4+IL-17A+Th17 cells in (B) spleens and (D) inguinal lymph nodes (n = 3/group). Flow cytometry for Foxp3 (Treg) expression in (E) spleens and (G) inguinal lymph nodes of the control, EAMG, and curcumin-treated group (n = 3/group). Frequencies of CD4+CD25+Foxp3+ Treg cells in (F) spleens and (H) inguinal lymph (n = 3/group). (I–M) Serum IL-6, IL-17A, IL-23, IL-10 and TGF-β1 were measured by ELISA. (I–M) (n = 6/group). The data are representative of three independent experiments. The data were expressed as means ± SEM,*P < 0.05, **P < 0.01, ***P < 0.001, ns = not significant.

curcumin, which suggested that curcumin could protect the intestinal epithelial barrier.

2.6. Curcumin regulated the Th17/Treg balance in T-AChR-induced MG mice

To investigate whether curcumin protects against MG by regulating the Th17/Treg balance, we evaluated the frequency of CD4^{+} IL-17A^{+} Th17 cells (Fig. 5A and C) and CD4^{+} CD25^{+} Foxp3^{+} Treg cells (Fig. 5E and G) in splenocytes and lymph node cells isolated from curcumin-treated and untreated MG mice. As shown in Fig. 5B and D, T-AChR induced a significantly increase in Th17 cells, which was obviously decreased when treated with curcumin. However, the frequency of Tregs significantly decreased in T-AChR-induced MG mice but evidently increased after treatment with curcumin (Fig. 5F and H).

To further verify the changes in Th17/Treg balance, relevant cytokines secreted from Th17 and Treg cells were examined in this study. Compared to the EAMG group, curcumin significantly reduced the levels of the proinflammatory cytokines IL-6 ($P < 0.05$) and IL-17A ($P < 0.001$) in the blood (Fig. 5I–J). Curcumin-treated and EAMG groups did not differ significantly in IL-23 levels (Fig. 5K). Furthermore, the curcumin treatment group exhibited significantly increased levels of the anti-inflammatory cytokines IL-10 ($P < 0.05$) and TGF-β1 ($P < 0.05$) in the blood compared with the EAMG group (Fig. 5L-M). These findings strongly suggest that curcumin regulates Th17/Treg cells and exerts an anti-inflammatory effect in MG animal models.

3. Discussion

Curcumin has been proven to be neuroprotective and anti-inflammatory in both humans and animals; furthermore, curcumin is used to treat Huntington's disease [28], Alzheimer's disease [29], and cerebral ischemia [32]. Recent studies in rats have revealed that curcumin is a potential treatment for MG, but the underlying mechanisms are not well investigated. According to our study, curcumin alleviated the clinical symptoms of MG mice, which was consistent with previous reports [26]. In addition, curcumin altered the gut microbiota composition, increased SCFA-producing bacteria, reduced intestinal permeability, and regulated the Th17/Treg balance of T-AChR-induced MG mice.

The gut microbiota has been linked to MG in various preclinical and clinical studies [21,23,24,33–35]. Curcumin and its metabolites have been demonstrated to affect the gut microbiota [36]. Our findings have revealed that curcumin could restore the original gut microbial composition in T-AChR-induced MG mice and increase the abundance of a few important bacterial species. The gut microbiome of EAMG mice had a significantly lower abundance and diversity than that of control mice, these findings verified earlier findings in MG patients [23]. However, the disorders of the gut microbiota during EAMG were restored after treatment with curcumin, which mainly manifested as an increase in gut microbial diversity and richness.

Bacteroidetes and Firmicutes play critical roles in regulating host metabolism, preserving intestinal barrier integrity, maintaining immunocompetence, and defending against pathogen invasion [37]. At the phylum level, EAMG mice showed no significant changes in the relative abundance of Firmicutes and Bacteroidetes, which might be due to the small sample size of the study. However, EAMG mice showed a significantly higher abundance of Proteobacteria than the control group, which was consistent with earlier research findings [21,34]. Interestingly, curcumin treatment decreased the relative abundance of Proteobacteria in EAMG mice. At the genus level, T-AChR significantly enhanced the relative abundance of *Desulfovibrio* compared to the control group, which is consistent with a prior report [22]. *Desulfovibrio* bacteria have been reported to be associated with colonic inflammation and mucosal injury in patients with acute ulcerative colitis [38]. Interestingly, the relative abundance of *Desulfovibrio* in EAMG mice is obviously decreased when treated with curcumin, suggesting a protective effect against T-AChR-induced gut dysbiosis. In addition, curcumin significantly altered the composition of the gut microbiota in EAMG mice by increasing the abundance of *Oscillospira*, *Akkermansia*, and *Allobaculum*, which might be related to the clinical severity of MG [23]. *Oscillospira* can probably generate SCFAs such as butyrate, which is negatively correlated with the Lennon score and might be a candidate probiotic for MG [39]. It is well known that Akkermansia (Akk) is also a kind of bacteria that produces SCFAs, especially butyrate, which affects the human body's metabolic functions and immune response [40]. *Allobaculum* is a butyrate producer [41], which may be responsible for metabolic alterations and immunological modifications in treated EAMG mice that trigger anti-inflammatory responses. Overall, curcumin could restore gut microbiota dysbiosis by affecting the composition of bacteria that produce SCFA. According to most researchers, MG is associated with a disruption of the gut microbiota and its metabolic SCFA products [21–23]. By fermenting partial or nondigestible polysaccharides, the gut microbiota produces SCFAs, which significantly improve chronic inflammatory and autoimmune conditions [42]. Propionate and butyrate have been found to promote peripheral Treg generation [16]. We found that curcumin administration significantly increased butyrate levels in T-AChR-induced MG mice. Notably, there was a reduction in the butyrate-producing species *Oscillospira*, *Akkermansia*, and *Allobaculum*, which define gut dysbiosis in T-AChR-induced MG mice. Nevertheless, curcumin recapitulates the bacteria that produce butyrate, suggesting that butyrate is a beneficial product of the gut microbiota when curcumin is metabolized that may contribute to curcumin's alleviation of MG symptoms.

Dysbiosis of the gut microbiota may cause a permeable mucosal barrier, inducing excessive inflammatory responses and an imbalance of T cells, which has been found to be associated with rheumatoid arthritis [43], inflammatory bowel disease [44], MG [45] and others. In our study, high plasma levels of zonulin, LPS, and FD4, as well as reduced expression of Occludin in the colon, indicated significantly increased gut permeability in T-AChR-induced MG mice. Intestinal barrier function and tight junctions are regulated by zonulin [46] whose increased levels are related to immune dysregulation, genetic susceptibility, and loss of intestinal barrier function, which might be key factors in the pathogenesis of inflammation and autoimmunity [47]. We found that curcumin inhibited the T-AChR-induced upregulation of Proteobacteria and *Desulfovibrio*, which are considered to be major pathogenic bacteria expressing endotoxins [48,49]. The endotoxin LPS is a component of the cell wall that can increase gut permeability in gram-positive bacteria

[50]. It is therefore thought that the elevated abundance of Proteobacteria and *Desulfovibrio* and the increased level of LPS are responsible for triggering the inflammatory response in response to T-AChR stimulation. Moreover, the gut microbiota has a direct impact on intestinal permeability. The increase in endotoxin production by Proteobacteria and *Desulfovibrio* in the T-AChR-induced model group may lead to an impairment role in intestinal permeability. Accordingly, curcumin reduced gut permeability in T-AChR-induced MG mice, resulting in decreased plasma levels of FD-4, zonulin, and LPS, as well as increased colonic expression of Occludin. The mechanism by which curcumin reduces intestinal permeability remains unclear, whether it is due to cell-autonomous mechanisms or indirect modulation of Proteobacillus and *Desulfovibrio* bacteria. Moreover, the host's immune system interacts bidirectionally with its gut microbiota. The question of whether curcumin modulates gut microbiota and immune system composition in parallel, or which process is dominant in response to curcumin signals, needs to be explored further.

Patients and animal models with MG have been shown to have abnormalities in Treg and Th17 function or expression. Activated Th17 cells and their secreted cytokines are associated with anti-AChR antibody-mediated autoimmunity at neuromuscular junctions [51]. In addition, abnormal numbers and dysfunction of Tregs have been reported in MG patients [52,53]. In our results, according to ELISA analyses, curcumin partially restored the upregulation of IL-6 and IL-17A and the downregulation of IL-10 and TGF-β that was induced by T-AChR. Consistently, curcumin increased the frequency of $CD4^+$ $CD25^+$ $Foxp3^+$ Tregs and decreased the frequency of $CD4^+$ $IL-17A^+$ Th17 cells in spleens and inguinal lymph nodes. This shows that curcumin has the ability to restore the imbalance of Th17/Treg cells in T-AChR-induced MG mice. As a result, the host's immune system contributes to the beneficial effects.

There are several limitations to this research. The study's use of too few experimental animals makes it difficult to examine potential confounding variables, and experimental studies should be conducted without sex restriction and in both male and female animals, but we only studied female mice, which is one of its limitations. Another drawback is that, like most animal models, the EAMG model does not accurately represent human disease. Although this animal model has been used to develop medications for the treatment of MG, and they have been consistently approved by the U.S. Food and Drug Administration. As a result, it is anticipated that promising outcomes from using this animal model could be useful. The fact that mice and humans have different gut microbiomes is another drawback of using the mouse model; however, we observed similar changes in the gut microbiome at the lower taxonomic level. In the future, we might be able to obtain insight into the functional activity of these bacteria through whole microbial transcriptome analysis. Further research is needed to investigate the signaling pathways and targets that curcumin uses to improve gut barrier function and alter the gut microbiota and its metabolites.

4. Conclusion

In summary, curcumin may protect mice against MG by modulating both gut microbiota and SCFAs levels, improving gut permeability, and regulating Th17/Treg balance. This study provides novel insights into curcumin's clinical value in MG therapy.

5. Material and methods

5.1. Experimental animals

C57BL/6J mice (female, 8 weeks old) were purchased from Vital River Laboratories (Beijing, China). The mice were raised in an SPF-class, temperature-controlled room (22 °C–23 °C) with a 12:12-h light-dark cycle. The Animal Care and Use Committee of Lanzhou University Second Hospital approved our study protocols related to mice (No D2021-095).

5.2. Establishment of the experimental autoimmune myasthenia gravis (EAMG) model

We immunized each mouse with *Torpedo californica* AChR (T-AChR) purified from the electric organ of *Torpedo californica* as previously described [54]. In detail, on day 0, we injected both hind footpads with an equal amount of Complete Freund's Adjuvant (CFA), and 30 μg of T-AChR was emulsified in 100 μL of PBS. The mice were immunized a second time by giving identical doses of T-AChR in Incomplete Freund's Adjuvant (IFA) at the base of the tail and in the back, separated by four-week intervals. CFA and IFA emulsions devoid of T-AChR were similarly administered to control mice.

5.3. Evaluation of EAMG symptoms

The mice were weighed on day 0 and twice a week during the experiment. The Lennon score was used to evaluate the severity of EAMG. Symptoms including tremors, stooped posture, muscular strength, and fatigability (30 s with repetitive paw grips on the cage grid) were used for clinical scoring. Grades of disease severity were assigned according to the following criteria: grade 0, normal strength and no abnormalities; grade 1, mildly decreased activity; grade 2, clinical signs present before exercise (tremors; head tilted downward; hunched posture; and a weak grip); grade 3, severe clinical signs present before exercise; and grade 4, dead. The findings are presented as the mean assessment value for each group of animals that was recorded at each time point [55].

5.4. Curcumin treatment

Curcumin was purchased from Sigma (Aldrich, St. Louis, MO, USA). Curcumin gavage was administered to animals in the curcumin intervention group at a dose of 100 mg/kg (prepared with 0.5% dimethyl sulfoxide (DMSO)) once a day [56]. The control group and

the MG model group were administered the corresponding volume of 0.5% DMSO for 4 weeks (from day 14–42).

5.5. Open field test (OFT)

In previous studies, the OFT was used to determine how the "MG gut microbiota" affects the host's locomotion ability [23,57]. The mice were moved to the detection room for approximately 30 min prior to the experiment. Two observers who conducted the behavioral test were unaware of the animal genotypes. A video-computerized tracking system (Smart, Panlab, Barcelona, Spain) was used to videotape behavioral assessments and quantify them [58].

In an open field setup with a white square base (45×45 cm^2) and blue walls (45 cm in height), every mouse was evaluated separately. The video-computerized tracking system captured all spontaneous activity for 5 min after gently placing a mouse in the center of the room for 1 min. A locomotion capacity index was calculated using the total motion distance [59].

5.6. Intestinal permeability detection

FITC-dextran 4 kDa (FD4) was measured to evaluate intestinal barrier permeability as previously described [60]. Briefly, after 6 h of starvation, the mice were administered FITC-dextran 4000 Da (Sigma, 44 mg/100 g body weight) (MW 4000; FD4, Sigma–Aldrich Co.) by oral gavage with a needle attached to a 1 ml syringe. Then, mice were sacrificed 4 h later, and blood was collected using a cardiac puncture; the blood was subsequently separated by centrifugation. The concentration of FITC-dextran was measured using multifunctional continuous spectroscopy (Thermo Fisher, USA) at excitation and emission wavelengths of 490 nm and 520 nm, respectively. In addition, plasma intestinal fatty acid binding protein (I-FABP), lipopolysaccharide (LPS), and zonulin were analyzed using commercial ELISA kits (NeoBioscience, China) according to the manufacturer's instructions. A microplate reader (Thermo Scientific, USA) was used to measure absorbance at 450 nm.

5.7. Quantitative RT–PCR

Total RNA was extracted from colon tissues using TRIzol reagent (Sigma–Aldrich), followed by reverse transcription to cDNA using the PrimeScriptTM RT reagent kit with gDNA Eraser (Takara Bio, Beijing, CHINA) according to the manufacturer's instructions. CDNA was normalized to the same concentration. Diluted cDNAs were used for real-time PCR with TB Green® Premix Ex Taq™ II (Takara Bio, Beijing, CHINA) on a bioanalyzer (Roche LightCyler96, IN). The relative mRNA expression of target genes was determined and normalized to the GAPDH RNA reference using the $2^{-\Delta\Delta CT}$ method. The primer sequences of Occludin sense 5′ - CCT CCA ATG GCA AAG TGA AT -3′ and anti-sense 5′ - CTC CCC ACC TGT CGT GTA GT -3′; ZO-1 sense 5′ - CCA CCT CTG TCC AGC TCT TC -3′ and anti-sense 5′ - CAC CGG AGT GAT GGT TTT CT -3′; GAPDH sense 5′ - ACA GTC CAT GCC ATC ACT GCC -3′ and anti-sense 5′ - GCC TGC TTC ACC ACC TTC TTG -3′.

5.8. Measurement of cytokine concentrations

Serum samples were collected, and cytokine levels of interleukin (IL)-6, IL-10, IL-17A, IL-23, and transforming growth factor-beta 1 (TGF-β1) were measured using a commercially available ELISA kit (NeoBioscience, China) according to the manufacturer's instructions.

5.9. Intracellular cytokine staining and Flow cytometry

Briefly, at day 42 after immunization, a single-cell suspension from the spleens and inguinal lymph nodes of each group of mice was prepared using a 70-mm cell strainer. After centrifugation, red blood cells (RBCs) were lysed using Red Cell Lysis Buffer (Sigma–Aldrich). Then, the lymphocytes were immunostained with cell surface markers and incubated in FACS buffer (PBS, 1 mM EDTA, 0.1% azide, and 1% BSA) for 30 min at 4 °C. For intracellular cytokine staining, the lymphocytes were stimulated for 4 h with a mixture of PMA (50 ng/mL), ionomycin (1 mg/mL), and monensin (2 mg/mL) (Sigma–Aldrich, St. Louis, MO, USA). Intracellular cytokine and Foxp3 staining were carried out using an intracellular staining kit (eBioscience) following the manufacturer's instructions. FITC-conjugated CD4, PE-conjugated CD25, APC-conjugated IL-17A, and APC-conjugated FoxP3 were used as fluorescence-conjugated antibodies. Phenotypic analysis was performed on a BD FACS Canto2 and evaluated using FlowJo V.11 software (Tree Star, Inc. San Carlos, CA, USA). All antibodies used in FACS were obtained from BioLegend.

5.10. 16S rRNA sequencing of the gut microbiome

5.10.1. DNA extraction and sequencing

Fresh fecal pellets from each mouse were collected in sterile EP tubes and kept at −80 °C for further investigation. Briefly, the Omega fecal DNA small extraction kit (Omega, USA) was used to collect microbial DNA from the stool. The V3–V4 regions of the bacterial 16S rRNA gene were amplified using PCR and primers 338F (5′-ACTCCTACGGGAGGCAGCA-3′) and 806R (5′-GGAC-TACHVGGGTWTCTAAT-3′) [61]. PCR products (480 bp) were purified using the Omega Gel Extraction Kit (Omega, USA) and confirmed by electrophoresis on a 2% agarose gel. Using QuantiFluor-ST (Promega, USA) and paired-end sequences (2×250) on an Illumina MiSeq platform in accordance with the established methods, purified amplicons were measured.

5.10.2. Sequencing data analysis

Raw fastq files were demultiplexed and quality-filtered using QIIME2 (version 2019.7, https://docs.qiime2.org). Any site with more than three consecutive bases and an average quality score of 20 had its 250 bp reads truncated. Reads with unclear base calls or barcode/primer mistakes that were shorter than 50 bp were ignored. By using UCHIME (http://drive5.com/uchime), chimeric sequences were identified and excluded from further studies. Using VSEARCH (version 9.2, http://drive5.com/uparse/), with 97% similarity, the remaining high-quality sequences were grouped into operational taxonomic units. The α-diversity was measured using species diversity indices (Shannon, Simpson) and species richness indices (Chao and Observed species). Unweighted UniFrac methods were used to measure beta diversity, which was then reported by principal main coordinate analysis (PCoA).

5.11. Determination of fecal SCFA levels

Fresh fecal samples were collected and frozen in liquid nitrogen. Twenty milligrams of the fecal sample with 1 mL of phosphoric acid solution (0.5% v/v) was first homogenized and then exposed to ultrasonication for 5 min in an ice bath. An eppendorf tube was used to collect the suspension (0.1 mL), which was then combined with 0.5 mL of MTBE solution (0.3 mg/L of 2-methyl valeric acid as the internal standard), vortexed for 3 min, ultrasonically processed for 5 min in an ice bath and centrifuged for 10 min at 12000 g. We then combined the supernatants (0.2 mL) with an equivalent volume of MTBE solution (containing 0.3 mg/L of 2-methyl valeric acid) in a glass autosampler vial. An Agilent 7890B gas chromatograph equipped with a DB-FFAP column (30 mm length 0.25 mm i.d. 0.25 μm film thickness, J&W Scientific, USA) connected to a 7000D mass spectrometer was used to conduct the GC−MS analysis of SCFAs.

5.12. Statistical analysis

Data are presented as the mean ± SEM. All statistical analyses were performed using GraphPad Prism 9.1 (GraphPad Software, La Jolla, CA, USA). The data were analyzed using one-way analysis of variance (ANOVA), and Tukey's test was performed to identify significant differences between the groups. P value < 0.05 was considered statistically significant.

Data availability statement

The data are available from the corresponding author upon reasonable request.

Ethics statement

All animal experimental protocols were approved by the Institutional Animal Care and Use Committee of Lanzhou University Second Hospital (No D2021-095).

Additional information

No additional information is available for this paper.

CRediT authorship contribution statement

Jing Sun: Writing – original draft, Visualization, Methodology, Formal analysis, Data curation, Conceptualization. **Qinfang Xie:** Funding acquisition, Data curation. **Mengjiao Sun:** Methodology, Formal analysis. **Wenjing Zhang:** Validation, Methodology, Data curation. **Hongxia Wang:** Software, Methodology, Investigation. **Ning Liu:** Visualization, Resources, Investigation. **Manxia Wang:** Writing – review & editing, Supervision, Project administration.

Declaration of competing interest

The authors declare that they have no known competing financial interests or personal relationships that could have appeared to influence the work reported in this paper.

References

[1] N.E. Gilhus, et al., Myasthenia gravis, Nat. Rev. Dis. Prim. 5 (2019) 30.
[2] J.A. Villegas, et al., An imbalance between regulatory T cells and T helper 17 cells in acetylcholine receptor-positive myasthenia gravis patients, Ann. N. Y. Acad. Sci. 1413 (2018) 154–162.
[3] A.T. Heldal, et al., Seropositive myasthenia gravis: a nationwide epidemiologic study, Neurology 73 (2009) 150–151.
[4] J.C. Deenen, et al., The Epidemiology of neuromuscular disorders: a comprehensive overview of the literature, J. Neuromuscul. Dis. 2 (2015) 73–85.
[5] J. Chen, et al., Incidence, mortality, and economic burden of myasthenia gravis in China: a nationwide population-based study, Lancet Reg Health West Pac 5 (2020) 100063.
[6] M.C. Dalakas, Immunotherapy in myasthenia gravis in the era of biologics, Nat. Rev. Neurol. 15 (2019) 113–124.
[7] J. Suh, J.M. Goldstein, R.J. Nowak, Clinical characteristics of refractory myasthenia gravis patients, Yale J. Biol. Med. 86 (2013) 255–260.
[8] S. Berrih-Aknin, Myasthenia Gravis: paradox versus paradigm in autoimmunity, J. Autoimmun. 52 (2014) 1–28.
[9] A. Marx, et al., Thymus and autoimmunity, Semin. Immunopathol. 43 (2021) 45–64.
[10] Y. Jiao, et al., Crosstalk between gut microbiota and innate immunity and its implication in autoimmune diseases, Front. Immunol. 11 (2020) 282.
[11] K. Atarashi, et al., ATP drives lamina propria T(H)17 cell differentiation, Nature 455 (2008) 808–812.
[12] K. Atarashi, et al., Induction of colonic regulatory T cells by indigenous Clostridium species, Science 331 (2011) 337–341.
[13] Ivanov II, et al., Specific microbiota direct the differentiation of IL-17-producing T-helper cells in the mucosa of the small intestine, Cell Host Microbe 4 (2008) 337–349.
[14] K. Atarashi, et al., Th17 cell induction by adhesion of microbes to intestinal epithelial cells, Cell 163 (2015) 367–380.
[15] Y. Furusawa, et al., Commensal microbe-derived butyrate induces the differentiation of colonic regulatory T cells, Nature 504 (2013) 446–450.
[16] N. Arpaia, et al., Metabolites produced by commensal bacteria promote peripheral regulatory T-cell generation, Nature 504 (2013) 451–455.
[17] M. Luu, A. Visekruna, Short-chain fatty acids: bacterial messengers modulating the immunometabolism of T cells, Eur. J. Immunol. 49 (2019) 842–848.
[18] W. Chen, et al., Artemisinin ameliorates the symptoms of experimental autoimmune myasthenia gravis by regulating the balance of TH1 cells, TH17 cells and Treg cells, J. Biol. Regul. Homeost. Agents 32 (2018) 1217–1223.
[19] J. Song, et al., Inhibition of ROCK activity regulates the balance of Th1, Th17 and Treg cells in myasthenia gravis, Clin. Immunol. 203 (2019) 142–153.
[20] F. Jing, et al., Rapamycin alleviates inflammation and muscle weakness, while altering the Treg/Th17 balance in a rat model of myasthenia gravis, Biosci. Rep. 37 (2017) BSR20170767.
[21] D. Qiu, et al., Altered gut microbiota in myasthenia gravis, Front. Microbiol. 9 (2018) 2627.
[22] G. Moris, et al., Fecal microbiota profile in a group of myasthenia gravis patients, Sci. Rep. 8 (2018) 14384.
[23] P. Zheng, et al., Perturbed microbial ecology in myasthenia gravis: evidence from the gut microbiome and fecal metabolome, Adv. Sci. 6 (2019) 1901441.
[24] X. Tan, et al., Differential gut microbiota and fecal metabolites related with the clinical subtypes of myasthenia gravis, Front. Microbiol. 11 (2020) 564579.
[25] M. Dei Cas, R. Ghidoni, Dietary curcumin: correlation between bioavailability and health potential, Nutrients 11 (2019) 2147.
[26] S. Wang, et al., Curcumin ameliorates experimental autoimmune myasthenia gravis by diverse immune cells, Neurosci. Lett. 626 (2016) 25–34.
[27] S.S. Patel, et al., Cellular and molecular mechanisms of curcumin in prevention and treatment of disease, Crit. Rev. Food Sci. Nutr. 60 (2020) 887–939.
[28] F. Labanca, et al., Therapeutic and mechanistic effects of curcumin in Huntington's disease, Curr. Neuropharmacol. 19 (2021) 1007–1018.
[29] S.K. Tiwari, et al., Curcumin-loaded nanoparticles potently induce adult neurogenesis and reverse cognitive deficits in Alzheimer's disease model via canonical Wnt/β-catenin pathway, ACS Nano 8 (2014) 76–103.
[30] W. Zam, Gut microbiota as a prospective therapeutic target for curcumin: a review of mutual influence, J Nutr Metab (2018) 1367984, 2018.
[31] H. Usuda, T. Okamoto, K. Wada, Leaky gut: effect of dietary fiber and fats on microbiome and intestinal barrier, Int. J. Mol. Sci. 22 (2021) 7613.
[32] Y. Ran, et al., Curcumin ameliorates white matter injury after ischemic stroke by inhibiting microglia/macrophage pyroptosis through NF-κB suppression and NLRP3 inflammasome inhibition, Oxid. Med. Cell. Longev. 2021 (2021) 1552127.
[33] C.S. Chae, et al., Prophylactic effect of probiotics on the development of experimental autoimmune myasthenia gravis, PLoS One 7 (2012) e52119.
[34] P. Liu, et al., Metagenome-wide association study of gut microbiome revealed potential microbial marker set for diagnosis of pediatric myasthenia gravis, BMC Med. 19 (2021) 159.
[35] A. Totzeck, et al., Gut bacterial microbiota in patients with myasthenia gravis: results from the MYBIOM study, Ther Adv Neurol Disord 14 (2021) 17562864211035657.
[36] B. Scazzocchio, L. Minghetti, M. D'Archivio, Interaction between gut microbiota and curcumin: a new key of understanding for the health effects of curcumin, Nutrients 12 (2020) 2499.
[37] S.M. Jandhyala, et al., Role of the normal gut microbiota, World J. Gastroenterol. 21 (2015) 8787–8803.
[38] F. Rowan, et al., Desulfovibrio bacterial species are increased in ulcerative colitis, Dis. Colon Rectum 53 (2010) 1530–1536.
[39] J. Yang, et al., Oscillospira - a candidate for the next-generation probiotics, Gut Microb. 13 (2021) 1987783.
[40] T. Zhang, et al., Akkermansia muciniphila is a promising probiotic, Microb. Biotechnol. 12 (2019) 1109–1125.
[41] B. Balakrishnan, et al., Prevotella histicola protects from arthritis by expansion of Allobaculum and augmenting butyrate production in humanized mice, Front. Immunol. 12 (2021) 609644.
[42] P. Gonçalves, J.R. Araújo, J.P. Di Santo, A cross-talk between microbiota-derived short-chain fatty acids and the host mucosal immune system regulates intestinal homeostasis and inflammatory bowel disease, Inflamm. Bowel Dis. 24 (2018) 558–572.
[43] G. Horta-Baas, et al., Intestinal dysbiosis and rheumatoid arthritis: a link between gut microbiota and the pathogenesis of rheumatoid arthritis, J Immunol Res 2017 (2017) 4835189.
[44] A. Nishida, et al., Gut microbiota in the pathogenesis of inflammatory bowel disease, Clin J Gastroenterol 11 (2018) 1–10.
[45] E. Rinaldi, et al., Gut microbiota and probiotics: novel immune system modulators in myasthenia gravis? Ann. N. Y. Acad. Sci. 1413 (2018) 49–58.
[46] L. Campisi, et al., Apoptosis in response to microbial infection induces autoreactive TH17 cells, Nat. Immunol. 17 (2016) 1084–1092.
[47] A. Fasano, Zonulin and its regulation of intestinal barrier function: the biological door to inflammation, autoimmunity, and cancer, Physiol. Rev. 91 (2011) 151–175.
[48] J. Ueyama, et al., Endotoxin from various gram-negative bacteria has differential effects on function of hepatic cytochrome P450 and drug transporters, Eur. J. Pharmacol. 510 (2005) 127–134.
[49] P. Xu, et al., Microbiome remodeling via the montmorillonite adsorption-excretion Axis prevents obesity-related metabolic disorders, EBioMedicine 16 (2017) 251–261.
[50] P. Kesika, et al., Role of gut-brain axis, gut microbial composition, and probiotic intervention in Alzheimer's disease, Life Sci. 264 (2021) 118627.
[51] A. Uzawa, et al., Roles of cytokines and T cells in the pathogenesis of myasthenia gravis, Clin. Exp. Immunol. 203 (2021) 366–374.
[52] A. Balandina, et al., Functional defect of regulatory CD4(+)CD25+ T cells in the thymus of patients with autoimmune myasthenia gravis, Blood 105 (2005) 735–741.
[53] S. Kohler, et al., CD4(+) FoxP3(+) T regulatory cell subsets in myasthenia gravis patients, Clin. Immunol. 179 (2017) 40–46.
[54] M. Robinet, et al., Use of toll-like receptor agonists to induce ectopic lymphoid structures in myasthenia gravis mouse models, Front. Immunol. 8 (2017) 1029.
[55] F. Baggi, et al., Breakdown of tolerance to a self-peptide of acetylcholine receptor alpha-subunit induces experimental myasthenia gravis in rats, J. Immunol. 172 (2004) 2697–2703.
[56] M.R. Afrin, et al., Curcumin reduces the risk of chronic kidney damage in mice with nonalcoholic steatohepatitis by modulating endoplasmic reticulum stress and MAPK signaling, Int. Immunopharm. 49 (2017) 161–167.
[57] E. Choleris, et al., A detailed ethological analysis of the mouse open field test: effects of diazepam, chlordiazepoxide and an extremely low frequency pulsed magnetic field, Neurosci. Biobehav. Rev. 25 (2001) 235–260.

[58] D. Yang, et al., Reduced neurogenesis and pre-synaptic dysfunction in the olfactory bulb of a rat model of depression, Neuroscience 192 (2011) 609–618.

[59] E.Y. Hsiao, et al., Microbiota modulate behavioral and physiological abnormalities associated with neurodevelopmental disorders, Cell 155 (2013) 1451–1463.

[60] L.C. Tong, et al., Propionate ameliorates dextran sodium sulfate-induced colitis by improving intestinal barrier function and reducing inflammation and oxidative stress, Front. Pharmacol. 7 (2016) 253.

[61] J. Wang, et al., Uncovering the microbiota in renal cell carcinoma tissue using 16S rRNA gene sequencing, J. Cancer Res. Clin. Oncol. 147 (2021) 481–491.